

ACCEPTED MANUSCRIPT • OPEN ACCESS

## The roles of global warming and Arctic Oscillation in the winter 2020 extremes in East Asia

To cite this article before publication: So-Hee Kim *et al* 2022 *Environ. Res. Lett.* in press <https://doi.org/10.1088/1748-9326/ac7061>

### Manuscript version: Accepted Manuscript

Accepted Manuscript is “the version of the article accepted for publication including all changes made as a result of the peer review process, and which may also include the addition to the article by IOP Publishing of a header, an article ID, a cover sheet and/or an ‘Accepted Manuscript’ watermark, but excluding any other editing, typesetting or other changes made by IOP Publishing and/or its licensors”

This Accepted Manuscript is © 2022 The Author(s). Published by IOP Publishing Ltd.

As the Version of Record of this article is going to be / has been published on a gold open access basis under a CC BY 3.0 licence, this Accepted Manuscript is available for reuse under a CC BY 3.0 licence immediately.

Everyone is permitted to use all or part of the original content in this article, provided that they adhere to all the terms of the licence <https://creativecommons.org/licenses/by/3.0>

Although reasonable endeavours have been taken to obtain all necessary permissions from third parties to include their copyrighted content within this article, their full citation and copyright line may not be present in this Accepted Manuscript version. Before using any content from this article, please refer to the Version of Record on IOPscience once published for full citation and copyright details, as permissions may be required. All third party content is fully copyright protected and is not published on a gold open access basis under a CC BY licence, unless that is specifically stated in the figure caption in the Version of Record.

View the [article online](#) for updates and enhancements.

1  
2  
3  
4  
5  
6  
7  
8  
9  
10  
11  
12  
13  
14  
15  
16  
17  
18  
19  
20  
21  
22  
23  
24  
25  
26  
27  
28  
29  
30  
31  
32  
33  
34  
35  
36  
37  
38  
39  
40  
41  
42  
43  
44  
45  
46  
47  
48  
49  
50  
51  
52  
53  
54  
55  
56  
57  
58  
59  
60

# The roles of global warming and Arctic Oscillation in the winter 2020 extremes in East Asia

So-Hee Kim<sup>1</sup>, V.N. Kryjov<sup>2</sup>, and Joong-Bae Ahn<sup>3</sup>

<sup>1</sup>Department of Atmospheric Sciences, BK21 School of Earth and Environmental Systems,  
Pusan National University, Busan, South Korea

<sup>2</sup>Research Institute for Basic Sciences, Pusan National University, Busan, South Korea

<sup>3</sup>Department of Atmospheric Sciences, Pusan National University, Busan, South Korea

\*Corresponding Author : **Joong-Bae Ahn**

Department of Atmospheric Sciences, Pusan National University

**2, Busandaehak-ro 63beon-gil, Geumjeong-gu, Busan, South Korea**

Phone: +82-51-514-1932

E-mail : [jbahn@pusan.ac.kr](mailto:jbahn@pusan.ac.kr)

Key words: climate extremes; Arctic Oscillation; global warming trend; statistical analysis

1  
2  
3  
4  
5  
6  
7  
8  
9  
10  
11  
12  
13  
14  
15  
16  
17  
18  
19  
20  
21  
22  
23  
24  
25  
26  
27  
28  
29  
30  
31  
32  
33  
34  
35  
36  
37  
38  
39  
40  
41  
42  
43  
44  
45  
46  
47  
48  
49  
50  
51  
52  
53  
54  
55  
56  
57  
58  
59  
60

## 26 Abstract

27 The 2019/20 winter was extremely warm globally and in the Northern Hemisphere  
28 extratropics. The main cause of climate extremes particularly in East Asia, was the extreme  
29 positive Arctic Oscillation (AO) event superimposed on steady global warming. The negligible  
30 trend in the AO over the preceding 41 years makes it possible to distinguish the roles of AO  
31 and global warming in the observed extremes. We estimate and compare contributions to  
32 January-March 2020 climate extremes by the AO and global warming represented by local  
33 temperature trends using the ERA5 reanalysis data. Based on results from a preliminary study,  
34 we estimate the contribution by global warming using linear regression while that by the AO  
35 using cubic regression, which is more restrained for the high AO index values than linear. The  
36 results show that the temperature extremes were mainly caused by the extreme positive AO  
37 event which accounts for approximately 3/4 of the observed temperature anomalies in northern  
38 East Asia and 2/3 in eastern East Asia. In southern East Asia, the AO contributes negligibly  
39 and positive temperature anomalies are related to global warming and local and regional  
40 impacts, particularly extreme SST, enhance south-westerlies and local radiative forcing.  
41 General conclusion is that the observed strong positive temperature anomalies including  
42 extreme anomalies over East Asia could have been achieved only as a combined effect of the  
43 extreme positive AO event and global warming. Quantification of the roles of the AO and  
44 global warming in climate extremes helps to estimate future anomalies caused by extreme AO  
45 events as well as assess uncertainties in climate model projections.

## 1. Introduction

The 2019/20 winter was the second warmest winter on 141-year record, with January-March (JFM) 2020 temperature anomaly being +1.15K for globe and +1.53K for the Northern Hemisphere against the 1901-2000 climatology (NOAA, 2020). Recent studies (Lawrence et al, 2020; Juzbašić et al., 2021) have shown that the winter 2019/20 climate extremes in the Northern extratropics were caused by an extremely positive Arctic Oscillation (AO) event. The AO recognized by Thompson and Wallace (1998; 2000) is a seesaw in sea level pressure (SLP) and geopotential height (GPH) anomalies between the polar region and the middle latitudes. In the lower troposphere, the positive AO phase is associated with the negative SLP and GPH anomalies encompassing the polar region and two stretched centers of the positive anomalies over the North Atlantic and North Pacific in the latitudinal belt 40°N-50°N. This pattern provides anomalous westerlies on the northern side of this positive anomaly belt and anomalous easterlies on its southern side. It is atmospheric circulation mode that dominates the wintertime climate over whole Northern Eurasia.

In East Asia, the 2019/20 winter was extremely warm, with observed wintertime temperatures being highest on record in Korea and Japan, with number and intensity of cold surges being anomalously low (figures are available at <https://data.kma.go.kr/climate/cdwv/selectCdwvDmap.do?pgmNo=733>). The mechanisms of the AO influence on East Asia temperature ensue from these AO-associated SLP/GPH anomaly patterns (Thompson and Wallace, 2000) and were discussed in previous studies (e.g., Thompson and Wallace, 2001; Wu et al., 2006; Park et al., 2011; Park and Ahn, 2016). The positive AO polarity associates with weakening of the Siberian High due to the enhanced heat advection with anomalous westerlies over Northern Eurasia, resulting in weakening of the East Asia Winter Monsoon (EAWM) (e.g., Gong et al., 2001), reducing of frequency, amplitude, and duration of cold surges (Zhang et al., 1997; Jeong and Ho, 2005; Park et al., 2011; Woo et al., 2012; Heo et al., 2018), and triggering the positive East Asia temperature anomaly (Gong et al., 2001). Also, the positive AO polarity associates with the anomalous heat advection from the ocean with the enhanced easterlies on the southern side of the North Pacific stretched center (e.g., Gong and Wang, 2003; Suo et al., 2009; Lee et al., 2013). Therefore, the described mechanisms suggest that a positive AO event can cause positive temperature anomalies in East Asia that provide the basis for our study focused on assessment of a portion of East Asia JFM 2020 observed positive extreme temperature anomalies caused by the extreme AO event and a portion associated with global warming.

The previous studies of the response to the extreme AO event have been focused on hemispheric or continental scale regions. Particularly, Lawrence et al. (2020) analyzes zonal mean temperature anomalies. They show that about two thirds of the zonal mean temperature

1  
2  
3  
4 84 anomalies in the latitudinal belt 40-70°N are linearly congruent with the AO index in JFM 2020,  
5 85 with the AO-congruent zonal mean positive temperature anomaly being largely contributed  
6 86 from western and north-eastern Eurasia with contribution from northern North America being  
7 87 negative (Lawrence et al., 2020, Fig. 6). However, the authors note that the quantity may partly  
8 88 be attributed to global warming because it was obtained on non-detrended data. Kryjov (2021)  
9 89 studies the separate linear contributions of the AO and global warming to the December-March  
10 90 2019/20 mean temperature anomalies over Northern Eurasia, focusing mainly on its western  
11 91 part, and reveals a dominant role of the AO enhanced by the trend components. However, the  
12 92 study has remained uncertainties because both the AO and trend contributions were estimated  
13 93 by linear models whereas some studies have suggested nonlinearity in local-scale temperature  
14 94 trends (e.g., Ribes et al., 2016) as well as in the temperature-AO relationships (e.g., Higgins et  
15 95 al., 2002; Son et al., 2012). Therefore, in this study, the appropriate functions representing the  
16 96 temperature trends and the temperature-AO relationships over East Asia are determined  
17 97 through preliminary studies. Kam et al (2022) show that 36% of December-February 2019/20  
18 98 mean Northwestern Russia temperature anomaly is linearly congruent with the North Atlantic  
19 99 Oscillation index. However, their result is not applicable to East Asia because the studied  
20 100 region is far distant from East Asia and zonal circulation was not strong in December (the AO  
21 101 index was 0.41).

22 102 Changes in weather and climate extremes occur regularly and it is evident that extremes of  
23 103 temperature will rise in the daily and seasonal time scales, and intermittent winter extremes  
24 104 will continue to appear (IPCC, 2014). Under these climate change, the Northern Eurasia Future  
25 105 Initiative (NEFI) ultimately seeks to develop a sustainable society by establishing appropriate  
26 106 mitigation and adaptation strategies accordingly through analysis of the changing climate and  
27 107 environment (Groisman et al 2017; Soja and Groisman, 2018). Located in the easternmost part  
28 108 of the NEFI domain, East Asia is a densely populated area where extreme climate greatly  
29 109 impacts social and economic status and development. Moreover, regional global warming  
30 110 wintertime manifestations in East Asia are strong and spatially inhomogeneous within the  
31 111 region (e.g., Jiang et al., 2004; Ahn et al., 2014; Xu et al., 2016; Luo et al., 2020). Therefore,  
32 112 quantification of the separate contributions of global warming and the AO to the extremes of  
33 113 2019/20 winter could increase our understanding of the forthcoming temperature extremes in  
34 114 East Asia. This not only provides a broader understanding of temperature extremes in the  
35 115 context of global warming but can also help regional decision makers in strategizing mitigation  
36 116 and adaptation. Along with daily mean temperature, we analyze the AO and global warming  
37 117 contributions to maximum and minimum temperatures

38 118 The purpose of the study is separation and quantification of the AO and global warming

1  
2  
3  
4 119 contributions to the JFM 2020 temperature extremes in East Asia accounting for possible  
5 120 nonlinearity of the local warming trends and temperature-AO relationships and their spatial  
6 121 inhomogeneity.  
7  
8

9 122 This paper is organized as follows. Section 2 describes the datasets and details the methods.  
10 123 Analysis of the 2020 regional climate anomalies and contributions by the AO and global  
11 124 warming are posted in Section 3. Discussion is in Section 4. Section 5 presents conclusions.  
12  
13  
14

15 125

## 16 126 **2. Data and Methods**

### 17 127 **2.1. Data**

18  
19  
20  
21 128 The monthly mean AO index (AOI) used is available from the Climate Prediction Center  
22 129 website at [https://www.cpc.ncep.noaa.gov/products/precip/CWlink/daily\\_ao\\_index/ao.shtml](https://www.cpc.ncep.noaa.gov/products/precip/CWlink/daily_ao_index/ao.shtml)  
23 130 (accessed 14 June 2021). It is updated monthly following the technology of Thompson and  
24 131 Wallace (2000) with the use of the 1000 hPa geopotential height (Z1000) fields poleward of  
25 132 20°N from NCEP-NCAR Reanalysis-1 (Kalnay et al., 1996) and the 1979-2000 basic period.  
26 133 Monthly mean indices are estimated by projecting monthly mean anomalies of Z1000 on the  
27 134 loading pattern that was estimated for the basic period as the first EOF of the year-round  
28 135 monthly mean Z1000 anomalies with respect to the corresponding monthly means weighted by  
29 136 square root of the cosine of latitude. All the AO monthly indices have the same loading pattern,  
30 137 and the published indices are not standardized that implies opportunity for estimation of the  
31 138 seasonal mean AOI values. This study focuses on January-March because the extreme seasonal  
32 139 mean AOI was observed during these months in 2020. It is important to note that the linear  
33 140 trend in the JFM AOI during the 41-year period (1979-2019), preceding the analyzed 2020,  
34 141 was negligible,  $0.01 \sigma/\text{year}$ , with 95% confidence intervals being  $0.03 \sigma/\text{year}$  (**Fig. 1**).  
35  
36  
37  
38  
39  
40  
41  
42  
43  
44  
45  
46  
47  
48  
49  
50  
51  
52  
53  
54  
55  
56  
57  
58  
59  
60

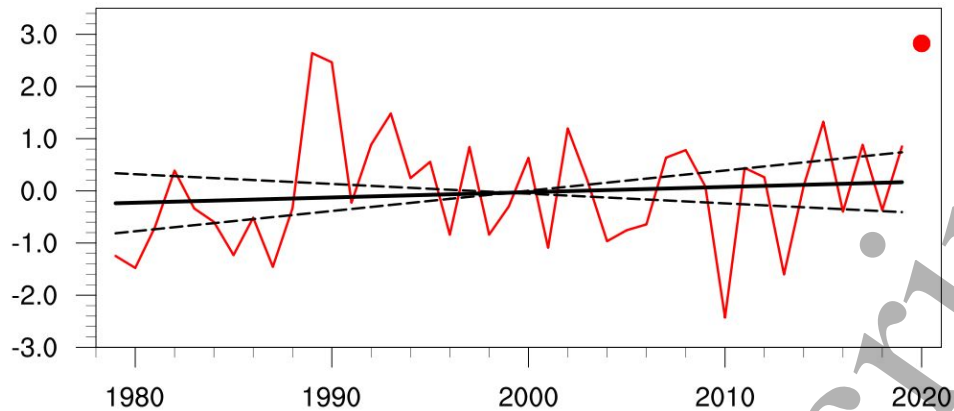


**Fig. 1.** The 1979-2019 time series of JFM AOI and its 41-year linear trend ( $0.01 \sigma/\text{year}$ , with 95% confidence intervals being  $0.03 \sigma/\text{year}$ ). The AOI value of JFM 2020 is shown with red dot.

A reasonable estimate of the contribution of the AO and global warming in East Asia would require high resolution long-term data sets covering up to JFM 2020. We selected the ERA5, a fifth-generation ECMWF reanalysis that covers data from 1979 to the present. The ERA5 reanalysis has a horizontal resolution of  $0.25^\circ \times 0.25^\circ$  and 37 vertical levels, it is available from the Copernicus Climate Change Service (C3S) Climate Data Store homepage (<https://cds.climate.copernicus.eu/cdsapp#!/search?type=dataset&text=era5>). The JFM mean temperature variables we use are seasonal means of daily mean (T2m), maximum (T2max), and minimum (T2min) temperature, obtained based on 1-hour data (Hersbach et al., 2018). Monthly data are additionally used in supporting analyses: SLP, sea surface temperature (SST), wind at 850hPa surface, surface net shortwave and long-wave radiation (Hersbach et al., 2019a; b). The monthly mean snow cover extent data were derived from the Rutgers University Global Snow Laboratory data meshed on the irregular  $88 \times 88$  grid.

## 2.2. Subregions of East Asia

The local manifestations of global warming as well as the AO impact on temperature essentially differs from each part of East Asia (**Fig. 2**). Particularly, the grid-points featuring statistically significant temperature trends are mainly concentrated in the southern part of East Asia and the adjacent seas (**Fig.2a**), whereas the AO influence is the strongest in the northern half of the East Asian region (**Fig. 2b**). Therefore, we divide the whole East Asia region into three subregions allowing more or less spatially homogeneous quantification of the contributions of global warming and the AO to the temperature extremes. Northern East Asia (NEA) is a subregion of comparatively low local temperature trends and of the strongest temperature response to the AO, mainly caused by variations in heat advection associated with

166 the AO. Eastern East Asia (EEA) is a subregion combining both significant temperature trends  
 167 and strong affect by the AO via its influence on the EAWM. Southern East Asia (SEA) is a  
 168 subregion of mainly significant local temperature trends and insignificant correlations of grid-  
 169 point temperatures with AOI.

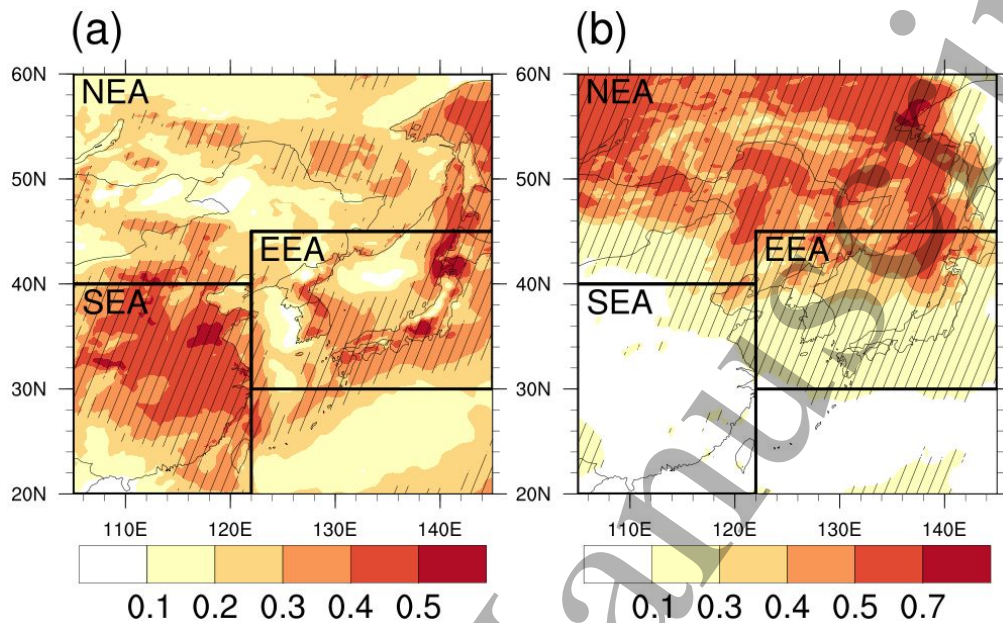


**Fig. 2.** Maps of (a) T2m trends based standardized T2m, and (b) coefficients of determination ( $R^2$ ) between the observed and estimated using cubic regression series of JFM T2m for 1979-2019. Rectangles show selected subregions of East Asia, Northern East Asia (NEA), Eastern East Asia (EEA), Southern East Asia (SEA). Please see details in the text. Thin nets mark the grid-points where (a) the linear trend and (b) correlation coefficient is significant at the 95% confidence level in two-tailed test.

### 2.3. Methods

We examined anomalies of the winter 2020 and the contributions of the AO and global warming to these anomalies with respect to climatology from 1979-2019. Global warming is characterized by the trend in globally averaged temperature or, that is the same under linear constraint at least, globally averaged local temperature trends. However, the local temperature trends, contributing to the global one, essentially differ from each other (e.g., IPCC, 2014, Fig. 1.1). So that, in our study, a grid-point manifestation of global warming was represented by a 1979-2019 local temperature trend (LTT) at this grid-point. Our preliminary analysis of the shape of the trend line for three selected subregions of East Asia with the use of linear, quadratic, and cubic polynomial approximations shows that for the analyzed 41-year period the linear approximation is the most appropriate based on  $F$ -value assessments. This result is supported



1  
2  
3  
4 183 by previous studies demonstrated that the non-linear trend with rapid temperature increase in  
5 184 the 1970s and restrained in the 2000s was the result of overlapping the global trends with  
6 185 natural variability, (Meehl et al., 2009; Zhou and Tung, 2013). Furthermore, Zhou and Tung  
7 186 (2013) showed that linear trend assessments for different recent time intervals within the past  
8 187 100 years vary insignificantly when overlapping variability was removed. For East Asia, the  
9 188 temperature trend nonlinear approximations underestimate the 2020 temperature value by  
10 189 several tenths of Kelvin as compared with linear for all three temperature characteristics, T2m,  
11 190 T2max, and T2min (**Fig. 3a-c and S1**). So that, our assessments could be considered as an  
12 191 upper bound of the global warming contribution for East Asia in JFM 2020.

13  
14  
15  
16  
17  
18 192 Son et al. (2012) documented nonlinearity in the temperature-AOI relationships. For the  
19 193 high and low AOIs some kind of “saturation” in temperature response occurs that results in  
20 194 overestimation of the temperature values associated with the high and low AOI values under  
21 195 linear constraints. Therefore, we performed preliminary analysis for East Asia and selected the  
22 196 cubic polynomial function as the most appropriate to characterize the temperature-AOI  
23 197 relationships (**Fig. 3d-f and S2**), with cubic regression coefficients being estimated separately  
24 198 for each grid-point.

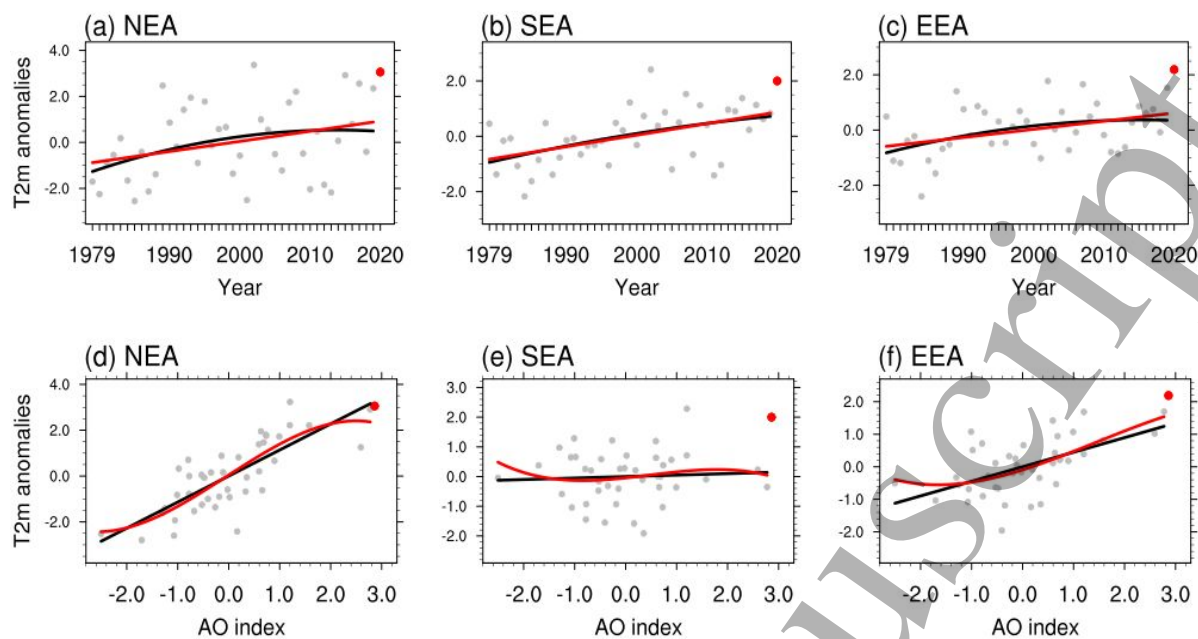


**Fig. 3. (Top)** JFM temperature time series (gray dots) from 1979-2019 for T2m for (a) NEA, (b) SEA, and (c) EEA (Unit: K). Linear trend derived on 1979-2019 time series is shown with red line; quadratic trend is shown with black line. The temperature values of JFM 2020 are shown with red dots; **(Bottom)** Scatterplots showing the temperature-AO relationships (gray dots) from 1979-2019 for T2m for (d) NEA, (e) SEA, and (f) EEA (Unit: K). Derived on 1979-2019 time series, cubic relationships are shown with red line, linear relationships are shown with black line. The temperature-AO relationship values of JFM 2020 are shown with red dots.

199

Since the linear trend in the AOI was negligible in 1979-2019, we consider the AOI and the grid-point linear temperature trend statistically independent during this period (we discuss this assumption in Section 4.1). In our study, the LTT and AO contributions are estimated by regression, with the training period being 1979-2019, with 2020 being the target year. For each grid-point we derive a regression equation for the LTT contribution using the grid-point original temperature time series as predictand and time as predictor. Then, we independently derive the cubic regression equation for the AO contribution on the grid-point linearly detrended time series, with the linear trend, although negligible, being subtracted from the AO indices as well. Significance of the regression coefficients was assessed by Student's *t*-statistic accounting for the effective series size (Bretherton et al., 1999). Since regression coefficients may be positive and negative, the appropriate confidence level was set at the 95% in two-tailed tests.

Following recommendations of Wilks (1995, p.311) we assess similarity between the patterns of observed temperature anomalies in JFM 2020 and patterns of the global warming

and AO contributions by spatial correlation coefficients. Accuracy of our statistical model is assessed by the root mean squared error (*RMSE*) between the JFM 2020 observed and estimated temperature fields. We compare the accuracy of representation of the observed temperature field by different estimated fields (the AO, LTT, AO+LTT contributions) by the mean squared skill score (*MSSS*), recommended by Murphy (1988):

$$MSSS = (MSE_{ref} - MSE_{ani})/MSE_{ref}$$

where *MSE* is the mean squared error of the observed temperature field representation by an estimated field, with the *MSE<sub>ani</sub>* corresponding to the analyzed estimated field and the *MSE<sub>ref</sub>* to the reference one. The *MSSS* is positive if the analyzed estimated field is closer to the observed one than the reference estimated field.

The statistical significance of the spatial correlation coefficients and *MSSS* values was assessed using a Monte Carlo resampling approach (Wilks, 1995). To account for the spatial correlation structure, we use the moving blocks procedure (Wilks, 1997). We estimated *p*-values by computing 1000 coefficients (*MSSS* values) between fields of randomly scrambled blocks of observations and unchanged contribution fields. We considered the spatial correlation coefficient (*MSSS*) significant at the 97.5% confidence level in one-tailed test if the *p*-value was below 2.5%.

### 3. Results

#### 3.1. Global Analysis of the AO and LTT Contributions to T2m anomalies of JFM 2020

As a preliminary analysis to provide a broader understanding of the results for East Asia we examine the AO and LTT contributions to the observed T2m anomalies of JFM 2020 on a global scale. **Fig 4a** shows an exceptionally warm winter in Northern Eurasia (anomalies exceed 5K), with East Asia anomalies exceeding 2K, positive anomalies of up to 2K over south-eastern North America, and negative anomalies of about -3K over Greenland and Alaska. The AO mainly contributes positively over western (exceeding 5K) and eastern (up to 5K) Northern Eurasia and negatively over Greenland (up to -5K). This spatial pattern of the AO contribution resembles the typical pattern of T2m anomalies associated with the positive AO events, although with stronger anomalies. The contribution of LTT is not spatially uniform. It is the largest over the Eastern Arctic (up to 5K) while over the continents it is mostly less than 2K. Areas of the largest underestimation of the JFM 2020 T2m anomalies are Western Siberia (residuals of up to 5K) and the Labrador Peninsula (residuals of up to 4K). The largest overestimation is over the Arctic Ocean (residuals are less than -5K) where both the AO and LTT contribute (incorrectly) positively based on the historical relationships

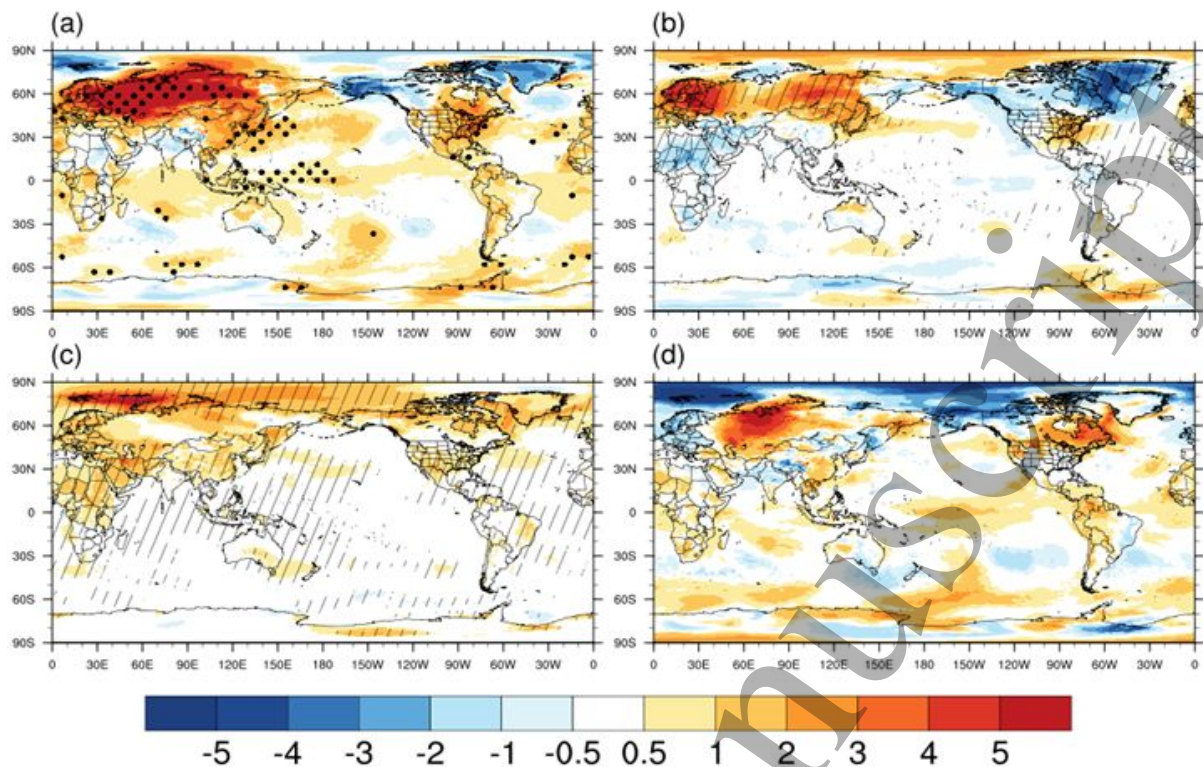


**Fig. 4.** (a) Anomaly of T2m in 2020 with respect to 1979-2019 climatology; black dots mark grid-points where T2m is the highest on record. (b) The AO contribution; thin nets mark the grid-points where the regression coefficient is significant at the 95% confidence level in two-tailed test. (c) The LWT contribution; thin nets mark the grid-points where the linear trend is significant at the 95% confidence level in two-tailed test. (d) The residual of the T2m anomaly in 2020 excluding the AO and LWT contributions (Unit: K).

248

249

### 3.2. Regional/subregional portion of the JFM 2020 anomalies congruent with the AO and global warming.

**Table 1** shows the portion of the JFM 2020 observed anomalies congruent with the AO and global warming. For whole East Asia, the average AO contribution accounts for 58% of T2m anomalies, while the LTTs contribute 32%, together they explain 90% of the observed anomalies. Over NEA, the AO portion increases up to 78%, while the global warming contribution accounts for 32%. Summation of these two contributions leads to 10% overestimation of the observed anomalies and essential negative residuals. EEA demonstrates results closest to the observations, 94% of the observed anomalies are congruent with the joint AO and global warming contribution, with the AO accounting for 66% and LTTs for 28%. The poorest results are for SEA, 45% of jointly explained portion of the observed anomaly, with the AO portion being 3% and the global warming portion being 42%. In general, our statistical model, implying contributions by only the AO and global warming, is appropriate for East Asia

on regional scale and on the subregional scale for NEA and EEA, for which residuals are about 10% of the observed anomaly. For SEA, where the AO influence is uncertain (**Fig. 3**), the only LTTs underestimate anomalies and remain large residual discussed in section 4.2. Results for T2max and T2min resemble those for T2m and are shown in Supplementary material (Table S1).

**Table 1.** Regional/subregional JFM 2020 mean observed T2m anomalies and their portions contributed by the AO, LTT, AO+LTT. The positive (negative) residuals correspond to underestimation (overestimation) of the observed anomalies.

Region /subregion	Mean anomaly (K)	Portion of observed anomaly (%) contributed by			Residual (%)
		AO	LTT	AO+LTT	
EA	2.35	58	32	90	10
NEA	3.02	78	32	110	-10
EEA	2.17	66	28	94	6
SEA	1.97	3	42	45	55

### 3.3. Particular temperature anomalies and contributions over East Asia

The positive T2m anomalies exceeding 2K over the land and 1K over the seas span almost whole East Asia (**Fig. 5a**), with new records being established in the northernmost NEA (anomalies exceed 5K in the Lena-Aldan interfluvium), most of EEA (anomalies of up to 4K), and coastal areas of SEA, (anomalies of up to 3K). The AO contributes positively (1K to 5K) over NEA and EEA (**Fig. 5b**). However, the AO positive contribution over SEA is negligible and even locally negative as a result of the low coefficient of determination ( $< 0.1$ ) between observed and estimated T2m (**Fig. 2b**). The LTTs contribute positively over whole East Asia, with contribution of 1K to 2K spanning SEA and parts of NEA and EEA (**Fig. 5c**). Regionally, the AO contribution is the strongest over NEA and weakest over the SEA, while LTTs' is relatively strong over SEA.



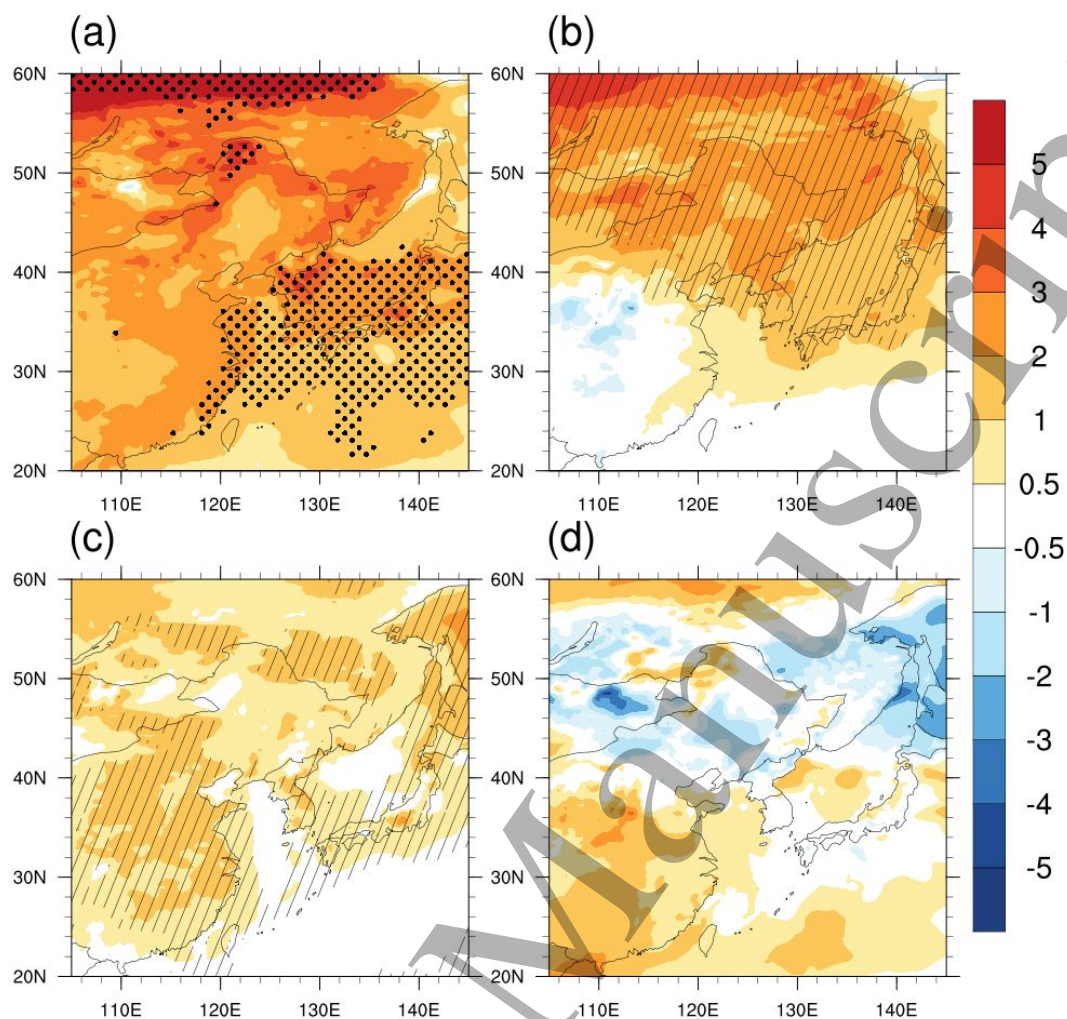


**Fig. 5.** Same as Fig. 4, but for East Asia.

287

288 As shown in Fig. 5d, the statistical model underestimates observed anomalies over SEA  
 289 (residuals of up to 2K) and over the Lena-Aldan interfluve and Manchuria in NEA (residuals  
 290 of up to 3K and 2K). Meanwhile, in the rest of NEA, residuals, mainly negative, are quite small  
 291 and randomly dispersed over land while the main area of the negative residuals (overestimation)  
 292 is over the adjacent seas. Over EEA, residuals do not exceed 1K, with residuals less than 0.5K  
 293 spanning the Korean Peninsula and Japanese Archipelago where the observed anomaly  
 294 extremes achieve 4K being the highest on record. The detail discussion on the residuals is  
 295 posted in the Section 4.3. For T2min and T2max, the results are similar to those of T2m. Please  
 296 refer to the supplementary material for details (**Figs. S3 and S4**).

297

### 3.4. Consistency between the observed and estimated temperature fields

Spatial correlation between the observed T2m field and the field estimated using the LTT is 0.38 while that estimated using AOI is 0.72, that indicates that the AO contribution pattern is closer to the observed anomaly pattern than the LTT contribution.

The *RMSE* for the T2m field estimated using the LTT (1.95K) is larger than that associated with the AO (1.34K) that supports the result from the consistency assessment on the superiority of the AO contribution. Superiority of the AO contribution also results from the significant positive *MSSS* value (0.53) assessing consistency between the observed field and the AO contribution in respect to the LTT contribution. However, the lowest *RMSE* (1.00K) is between the observed field and the field combining both the AO and LTT contributions, meanwhile, the significant positive *MSSS* value (0.45) proves that it is global warming that essentially improves the field estimated based on the AO alone. The field consistency scores for T2min and T2max are similar to those obtained for T2m, see **Tables S2** and **S3** in Supplementary material for detailed values. Consequently, the observed strong positive temperature anomalies including extreme anomalies over East Asia could have been achieved only as a combined effect of the extreme positive AO event and global warming.

## 4. Discussion

### 4.1. Relationships between the AO and global warming

Our study is based on assumption of statistical independence between AOI and global warming trend over the 41-year training period during which the AOI trend was negligible. Meanwhile, statistical independence during a certain period does not imply physical independence between the AO and global warming. Particularly, at least two physically plausible mechanisms linking the AO and global warming that offset each other have been suggested. The first mechanism has been detailed and supported in the model studies by Shindell et al. (2001). Increase of well mixed greenhouse gas concentration in atmosphere results in increase in horizontal temperature gradient between the upper tropical troposphere and lower polar stratosphere that results in enhancement of the polar vortex, that is, the positive AOI polarity. The second suggested mechanism is based on the Arctic amplification, the enhanced Arctic warming as compared with the middle and lower latitudes caused by the positive feedback between the sea ice retreat and global warming. It must result in decrease of the temperature gradient between middle and polar latitudes, enhancement of meridional circulation and weakening of zonal one, that is, in the negative AOI polarity (Cohen et al., 2020, and references therein). However, it should be noted that there is no consensus on the second mechanism yet, with model studies disagreeing each other and observed periods being

1  
2  
3  
4 333 too short for reliable statistical confirmation (Cohen et al., 2020). The first mechanism  
5 334 prevailed in the 1960s-1990s, with the AOI trend during 1959-1997 being  $0.041 \pm 0.032\sigma/\text{year}$ .  
6 335 Associated significant contribution to the global warming signals during the 1960s-1990s was  
7 336 demonstrated by Thompson et al. (2000) and numerous following studies. However, since the  
8 337 1990s, the AOI trend has been decreasing down to the negative values (Kryzhov and Gorelits,  
9 338 2015), and the AO signal became distinguishable from that of global warming (Cohen and  
10 339 Barlow, 2005). This AOI decrease was possibly caused by the second mechanism.

11  
12  
13  
14  
15 340 Our training period comprises both the AOI positive and negative trend periods, with the  
16 341 AOI trend for the whole 41-year training period turning out negligible. We should note that  
17 342 external forcings not related to global warming that may also affect the AO have been also  
18 343 suggested, particularly, variations in ultra-violet solar radiation and volcano eruptions (e.g.,  
19 344 Shindell et al., 2001). Therefore, if the AOI trend were significant, uncertain would be the  
20 345 causes of the trend, and the AO signal would become undistinguishable from that of global  
21 346 warming in an empirical study. Meanwhile, for the period 1979-2019 when the AO trend is  
22 347 negligible, the AO and global warming signals become distinguishable, so do their  
23 348 contributions to the anomalies of JFM 2020.

24  
25  
26  
27  
28  
29  
30 349 We have also analyzed status of the snow cover extent (SCE) of JFM 2020 which may  
31 350 influence on the AO and East Asia temperature at the same time. As has been shown by  
32 351 Juzbašić et al. (2021) development of the extreme positive JFM AO event was abnormal in the  
33 352 autumn and winter of 2019/20. It was preceded by enlarged October and November SCE in  
34 353 Eastern Eurasia that tends to result in the negative AO phase rather than positive (Cohen et al.,  
35 354 2007; Cohen and Jones, 2011; Han and Sun, 2018). However, in spite of the extreme positive  
36 355 JFM AO event, because of its abnormal development, the autumn 2019 area averaged SCE  
37 356 anomaly standardized in respect to 1979-2019 was 0.95 in East Asia. The positive SCE  
38 357 anomaly persisted into winter being 0.56 in JFM 2020, weakening the AO-induced warming  
39 358 impact. Meanwhile, the East Asia JFM SCE negatively correlates with the AO with coefficient  
40 359  $-0.44$  on the detrended 41-year series.

41  
42  
43  
44  
45  
46  
47 360 It is also worth noting that the positive SST anomalies in the equatorial Pacific, with the  
48 361 JFM 2020 Nino3.4 index being 0.5, similarly to the autumn positive SCE anomalies in Eastern  
49 362 Eurasia, were favorable for the negative phase of the AO (Fletcher and Cassou, 2015) rather  
50 363 than the extreme positive AO event

51  
52  
53  
54 364



## 4.2. Residuals

Temperature anomalies are overestimated (negative residuals) by 10% as average over NEA, with the largest negative residuals spanning the seas as a result of underestimation of enhanced cold advection from the continent with anomalous westerlies and prevailing negative SST anomalies (**Figs. 6a and S5**). The negative residuals in the continental area may be a result from the positive SCE anomaly in NEA, with standardized in respect to 1979-2019 area average SCE anomaly in JFM 2020 being 0.75. On the background of average overestimation, there are two areas of essential underestimation of the observed anomalies those are the northernmost NEA part and the central NEA part over Manchuria. The northernmost area of NEA in JFM 2020 was affected by anomalous westerlies in the western part and southerlies in the eastern part (**Fig. S5**), which caused additional heat advection from warmer western domain and from the East Sea (**Figs. 4d and 6a**), not inherent in the classical AO pattern, and could result in the underestimation of anomalies by the model. It should be noted that SST of the East Asia adjacent seas was extremely high in JFM 2020 (**Fig. 6a**) in contrast to the negative SST anomaly in 1989 when the previous extreme AO event occurred (Juzbašić et al., 2021). The area of the positive residuals in Manchuria is a comparatively flat valley bordered in the north with an arc of the trans-Baikal ridges opened to anomalous south-easterlies of JFM 2020 (**Fig. S6**). Also, these positive residuals could result from an anomalous radiative forcing during JFM 2020 (**Fig. 6b**) that corresponds to the enhanced role of radiative forcing in temperature variability in the dryland belt (Groisman et al., 2018).

Underestimation by 40-69% of the observed anomalies over SEA, at least in its eastern part where anomalies were extreme, was caused by the anomalous heat advection to the region from the adjacent seas with extremely high SST (**Figs. 6a and S5**). Given that the tendency of a weaker winter monsoon marked by warmer winters to occur in El Niño years (Ha et al., 2012), the extremely high SST could be related to a weak El Niño during JFM 2020. However, both low intensity of El Niño (Nino3.4 index was 0.5) and rather low mosaic distributed correlation between SST in the adjacent seas and the Nino3.4 index, slightly exceeding the 95% confidence level (**Fig. S7**), do not imply a strong El Niño impact on East Asia T2m in JFM 2020. Meanwhile, in the north-western continental part anomalous radiative forcing (**Fig. 6b**) could explain essential underestimation of the observed anomalies by the LTT alone with no additional contribution by the AO.

Analysis of residuals, that is, the portion of the observed anomalies not dominated by global warming and the AO, with both impacts being parameterized on the 1979-2019 series, reveals that the residuals were mainly caused by extremely high SST of the seas adjacent to East Asia, anomalous south-easterlies, and locally anomalous radiative forcing.

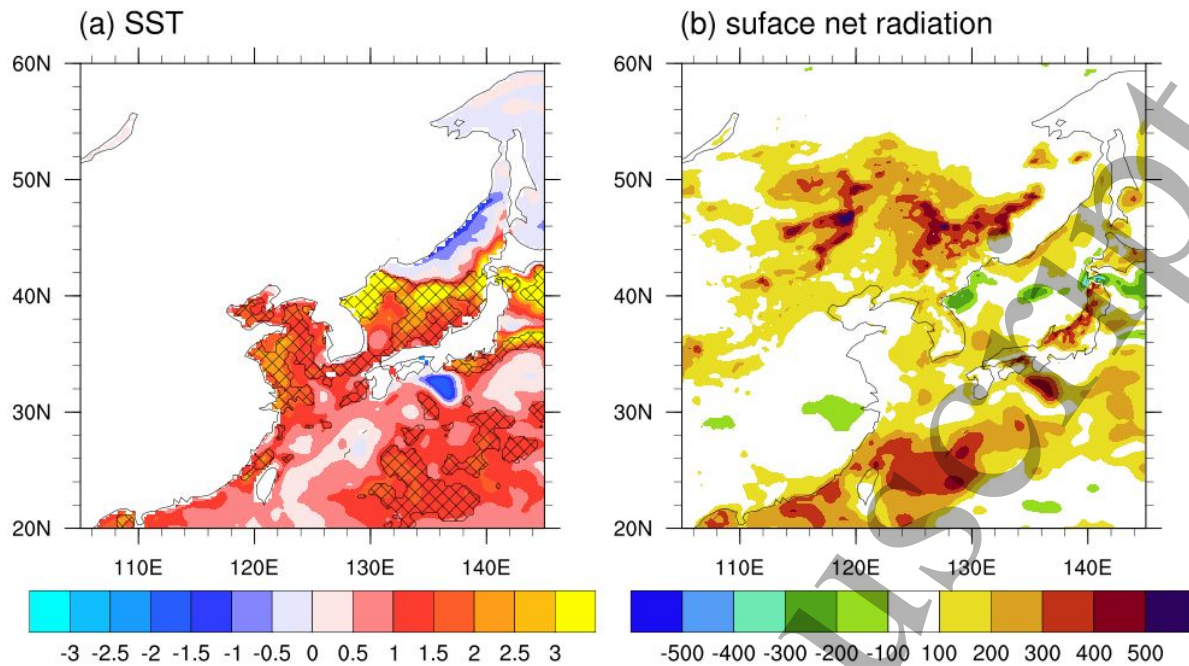


**Fig. 6.** Anomalies of (a) SST (Unit: K) and (b) surface net radiation (Unit:  $\text{W}/\text{m}^2$ ) in JFM 2020 with respect to 1979-2019 climatology. Thin nets in (a) mark grid-points where SST is the highest on record. The value in (b) was calculated as an algebraic sum of mean surface net shortwave and longwave radiation flux, the positive indicates downwards.

400

401

## 5. Conclusion

In recent decades, the occurrences of abnormally high temperatures have increased in frequency and intensity. Global warming caused by Earth's radiative imbalance clearly contributes to this, but its local manifestations are not uniform. It raises the question of whether each new regional temperature extreme is a result from global warming or regional peculiarities, particularly anomalous heat advection with circulation anomalies. The extremely warm winter of 2019/20 gave us a unique opportunity to compare the roles of global warming and the AO in achieving these extremes based on observations.

We performed this analysis for East Asia based on linear LTTs and cubic temperature-AO relationships. The extremely positive AO event accounts for 78% and 66% of the temperature extremes in NEA and EEA, correspondingly, and had a negligible effect for SEA. Moreover, the LTTs made the anomaly patterns estimated by the AO contributions more consistent with those observed in all regions. Notably, the LTTs account for 42% of the anomalies observed in SEA. Meanwhile, the statistical model in this study showed residuals in some regions of NEA and SEA, which appear to be related to the unique climate features of JFM 2020, such as

1  
2  
3  
4 417 anomalously high SLP over the Northern Pacific and associated anomalous heat advection to  
5 418 East Asia, extremely warm SST along the East Asia coast, and enhanced radiative forcing over  
6 419 Manchuria.

7  
8  
9 420 This study suggests that the 2020 wintertime temperature extremes would probably not  
10 421 have occurred in the absence of either the extreme AO event or background global warming  
11 422 and shows that superimposing of certain climate modes on global warming could lead to  
12 423 previously unexperienced extremes in future. These results have implications for the evaluation  
13 424 of possible temperature anomalies caused by the extreme AO events behind steady climate  
14 425 system changes, particularly the temperature's upward trend which matches the goals of NEFI  
15 426 (Groisman et al 2017; Soja and Groisman, 2018). It also suggests that appropriate climate  
16 427 change adaptation and mitigation should be implemented as soon as possible in East Asia, as  
17 428 the occurrence of extreme events in response to climate change might pose challenges to  
18 429 sustainable societies.

19 430

## 20 431 **Acknowledgments**

21 432 This work was funded by the Korea Meteorological Administration Research and  
22 433 Development Program under Grant KMI2020-01411.

23 434 ERA5, a fifth-generation ECMWF reanalysis data (Hersbach et al., 2018; 2019a; b) are  
24 435 provided by the Copernicus Climate Change Service (C3S) and were obtained from Climate  
25 436 Data Store (CDS) homepage at <https://cds.climate.copernicus.eu/>. Monthly AO indices are  
26 437 taken from the NOAA Climate Prediction Center website (<https://www.cpc.ncep.noaa.gov/>).  
27 438 Snow cover data were provided by Rutgers University  
28 439 (<https://climate.rutgers.edu/snowcover/index.php>)

29 440

## 30 441 **Data availability statement**

31 442 The data that support the findings of this study are available upon request from the authors.

## References

- Ahn, J.-B., Choi, Y.-W., Jo, S. & Hong, J.-Y. (2014). Projection of 21st century climate over Korean Peninsula: temperature and precipitation simulated by WRFV3. 4 based on RCP4. 5 and 8.5 scenarios. *Atmosphere*, 24(4), 541-554. <https://doi.org/10.14191/Atmos.2014.24.4.541>
- Bretherton, C. S., Widmann, M., Dymnikov, V. P., Wallace, J. M. & Bladé, I. (1999). The effective number of spatial degrees of freedom of a time-varying field. *Journal of climate*, 12(7), 1990-2009. [https://doi.org/10.1175/1520-0442\(1999\)012<1990:TENOSD>2.0.CO;2](https://doi.org/10.1175/1520-0442(1999)012<1990:TENOSD>2.0.CO;2)
- Cohen, J. & Barlow, M. (2005). The NAO, the AO, and Global Warming: How Closely Related?, *Journal of Climate*, 18(21), 4498-4513. <http://doi.org/10.1175/JCLI3530.1>
- Cohen, J., Barlow, M., Kushner, P. J., & Saito, K. (2007). Stratosphere-troposphere coupling and links with Eurasian land surface variability. *Journal of Climate*, 20(21), 5335-5343. <https://doi.org/10.1175/2007JCLI1725.1>
- Cohen, J., & Jones, J. (2011). A new index for more accurate winter predictions. *Geophysical Research Letters*, 38(21). <https://doi.org/10.1029/2011GL049626>
- Cohen, J., Zhang, X., Francis, J., et al. (2020). Divergent consensus on Arctic amplification influence on midlatitude severe winter weather. *Nature Climate Change*, 10, 20–29. <https://doi.org/10.1038/s41558-019-0662-y>
- Fletcher, C. G., & Cassou, C. (2015). The dynamical influence of separate teleconnections from the Pacific and Indian Oceans on the northern annular mode. *Journal of Climate*, 28(20), 7985-8002. <https://doi.org/10.1175/JCLI-D-14-00839.1>
- Gong, D. & Wang, S. (2003). Influence of Arctic Oscillation on winter climate over China. *Journal of Geographical Sciences*, 13(2), 208-216. <https://doi.org/10.1007/BF02837460>
- Gong, D. Y., Wang, S. W. & Zhu, J. H. (2001). East Asian winter monsoon and Arctic oscillation. *Geophysical research letters*, 28(10), 2073-2076. <https://doi.org/10.1029/2000GL012311>
- Groisman, P., Shugart, H., Kicklighter, D., et al. (2017). Northern Eurasia Future Initiative (NEFI): facing the challenges and pathways of global change in the twenty-first century. *Progress in Earth and Planetary Science*, 4(1), 1-48, <https://doi.org/10.1186/s40645-017-0154-5>
- Groisman, P., Bulygina, O., Henebry, G., et al. (2018). Dryland belt of Northern Eurasia: contemporary environmental changes and their consequences. *Environmental Research Letters*, 13(11), 115008, <https://doi.org/10.1088/1748-9326/aae43c>
- Ha, K.-J., Heo, K.-Y., Lee, S.-S., Yun, K.-S., & Jhun, J.-G. (2012). Variability in the East Asian

- 1  
2  
3  
4 480 Monsoon: a review. *METEOROLOGICAL APPLICATIONS*, 19(2), 200-215.  
5 http://doi.org/10.1002/met.1320  
6 481
- 7 482 Han, S., & Sun, J. (2018). Impacts of autumnal Eurasian snow cover on predominant modes of  
8 boreal winter surface air temperature over Eurasia. *Journal of Geophysical Research:*  
9 483 *Atmospheres*, 123(18), 10-076. <https://doi.org/10.1029/2018JD028443>  
10 484
- 11 485 Heo, J-W, Ho C-H, Park T-W, Choi W, Jeong J-H, & Kim J. (2018). Changes in Cold Surge  
12 Occurrence over East Asia in the Future: Role of Thermal Structure. *Atmosphere*, 9(6),  
13 486 222. <https://doi.org/10.3390/atmos9060222>  
14 487
- 15 488 Hersbach, H., Bell, B., Berrisford, P., et al. (2018). ERA5 hourly data on single levels from  
16 1979 to present. Copernicus Climate Change Service (C3S) Climate Data Store (CDS).  
17 489 <http://doi.org/10.24381/cds.adbb2d47>  
18 490
- 19 491 Hersbach, H., Bell, B., Berrisford, P., et al. (2019a). ERA5 monthly averaged data on pressure  
20 492 levels from 1979 to present. Copernicus Climate Change Service (C3S) Climate Data  
21 493 Store (CDS). <http://doi.org/10.24381/cds.6860a573>  
22 494
- 23 494 Hersbach, H., Bell, B., Berrisford, P., et al. (2019b). ERA5 monthly averaged data on single  
24 495 levels from 1979 to present. Copernicus Climate Change Service (C3S) Climate Data  
25 496 Store (CDS). <http://doi.org/10.24381/cds.f17050d7>  
26 497
- 27 497 Higgins, R. W., Leetmaa, A. & Kousky, V. E. (2002). Relationships between climate variability  
28 498 and winter temperature extremes in the United States, *Journal of Climate*, 15(13),  
29 499 1555–1572, [http://doi.org/10.1175/1520-0442\(2002\)015<1555:RBCVAW>2.0.CO;2](http://doi.org/10.1175/1520-0442(2002)015<1555:RBCVAW>2.0.CO;2)  
30 500
- 31 500 IPCC (2014). Climate Change 2014: Synthesis Report. Contribution of Working Groups I, II  
32 501 and III to the Fifth Assessment Report of the Intergovernmental Panel on Climate  
33 502 Change [Core Writing Team, R.K. Pachauri and L.A. Meyer (eds.)]. IPCC, Geneva,  
34 503 Switzerland, 151pp.  
35 504
- 36 504 Jeong, J.-H., and Ho, C.-H. (2005), Changes in occurrence of cold surges over east Asia in  
37 505 association with Arctic Oscillation, *Geophys. Res. Lett.*, 32, L14704,  
38 506 <http://doi.org/10.1029/2005GL023024>.  
39 507
- 40 507 Jiang, D. B., Wang, H. J. & Lang, X. M. (2004). East Asian climate change trend under global  
41 508 warming background. *Chinese Journal of Geophysics*, 47(4), 675-681.  
42 509 <https://doi.org/10.1002/cjg2.3536>  
43 510
- 44 510 Juzbašić, A., Kryjov, V. N. & Ahn, J.-B. (2021). On the anomalous development of the  
45 511 extremely intense positive Arctic Oscillation of the 2019-2020 winter. *Environ. Res.*  
46 512 *Lett.* 16(5), 055008. <https://doi.org/10.1088/1748-9326/abe434>.  
47 513
- 48 513 Kalnay, E., Kanamitsu, M., Kistler, R., et al. (1996). The NCEP/NCAR 40-year reanalysis  
49 514 project. *Bulletin of the American meteorological Society*, 77(3), 437-472.  
50 515 [https://doi.org/10.1175/1520-0477\(1996\)077<0437:TNYRP>2.0.CO;2](https://doi.org/10.1175/1520-0477(1996)077<0437:TNYRP>2.0.CO;2)  
51 516
- 52 516 Kam, J., Min, S., Kim, Y., Kim, B., & Kug, J. (2022). Anthropogenic Contribution to the  
53  
54  
55  
56  
57  
58  
59  
60

- 1  
2  
3  
4 517 Record-Breaking Warm and Wet Winter 2019/20 over Northwest Russia, *Bulletin of*  
5 518 *the American Meteorological Society*, 103(3), S38-S43.  
6 519 <https://doi.org/10.1175/BAMS-D-21-0148.1>.  
7  
8  
9 520 Kryjov, V. N. (2021). Climate Extremes of the 2019/2020 Winter in Northern Eurasia:  
10 521 Contributions by the Climate Trend and Interannual Variability Related to the Arctic  
11 522 Oscillation. *Russian Meteorology and Hydrology*, 46(2), 61-68.  
12 523 <http://doi.org/10.3103/S1068373921020011>  
13  
14 524 Kryzhov, V. N. & Gorelits, O. V. (2015) The Arctic Oscillation and its impact on temperature  
15 525 and precipitation in Northern Eurasia in the 20th century. *Russ. Meteorol. Hydrol.* 40  
16 526 711–721. <https://doi.org/10.3103/S1068373915110011>  
17  
18 527 Lawrence, Z. D., Perlwitz, J., Butler, A. H., Manney, G. L., Newman, P. A., Lee, S. H. & Nash,  
19 528 E. R. (2020). The Remarkably Strong Arctic Stratospheric Polar Vortex of Winter 2020:  
20 529 Links to Record-Breaking Arctic Oscillation and Ozone Loss. *Journal of Geophysical*  
21 530 *Research: Atmospheres*, 125(22), e2020JD033271.  
22 531 <https://doi.org/10.1029/2020JD033271>  
23  
24 532 Lee, S.-S., Kim, S.-H., Jhun, J.-G., Ha, K.-J. & Seo, Y.-W. (2013). Robust warming over East  
25 533 Asia during the boreal winter monsoon and its possible causes. *Environmental*  
26 534 *Research Letters*, 8(3), 034001. <http://dx.doi.org/10.1088/1748-9326/8/3/034001>  
27  
28 535 Luo, M., Feng, J. M., Xu, Z. F., Chen, L., Wang, J., Wang, Y. L., Lin, S. & Zhong, L. H.  
29 536 (2020). Decadal Wintertime Temperature Changes in East Asia During 1958–2001 and  
30 537 the Contributions of Internal Variability and External Forcing. *Journal of Geophysical*  
31 538 *Research: Atmospheres*, 125(14), e2019JD031840.  
32 539 <https://doi.org/10.1029/2019JD031840>  
33  
34 540 Meehl, G. A., Hu, A. & Santer, B. D. (2009). The Mid-1970s Climate Shift in the Pacific and  
35 541 the Relative Roles of Forced versus Inherent Decadal Variability. *Journal of Climate*,  
36 542 22(3), 780-792. <https://doi.org/10.1175/2008JCLI2552.1>  
37  
38 543 Murphy, A.H. (1988). Skill scores based on the mean squared error and their relationships to  
39 544 the correlation coefficient. *Monthly Weather Review*, 116(12), 2417–2424.  
40 545 [https://doi.org/10.1175/1520-0493\(1988\)116<2417:SSBOTM>2.0.CO;2](https://doi.org/10.1175/1520-0493(1988)116<2417:SSBOTM>2.0.CO;2)  
41  
42 546 NOAA National Centers for Environmental Information. (2020). State of the Climate: Global  
43 547 Climate Report for March 2020. <https://www.ncdc.noaa.gov/sotc/global/202003>.  
44  
45 548 Park, H.-J. & Ahn, J.-B. (2016). Combined effect of the Arctic Oscillation and the Western  
46 549 Pacific pattern on East Asia winter temperature. *Climate Dynamics*, 46(9-10), 3205-  
47 550 3221. <https://doi.org/10.1007/s00382-015-2763-2>  
48  
49 551 Park, T.-W., Ho, C.-H. & Yang, S. (2011). Relationship between the Arctic Oscillation and  
50 552 cold surges over East Asia. *Journal of climate*, 24(1), 68-83.  
51 553 <https://doi.org/10.1175/2010JCLI3529.1>  
52  
53  
54  
55  
56  
57  
58  
59  
60

- 1  
2  
3  
4 554 Ribes, A., Corre, L., Gibelin, A.-L. & Dubuisson, B. (2016). Issues in estimating observed  
5 555 change at the local scale – a case study: the recent warming over France. *International*  
6 556 *Journal of Climatology*, 36(11), 3794-3806. <https://doi.org/10.1002/joc.4593>  
7  
8 557 Shindell, D. T., Schmidt G. A., Miller R. L. & Rind D. (2001). Northern Hemisphere winter  
9 558 climate response to greenhouse gas, ozone, solar, and volcanic forcing. *Journal of*  
10 559 *Geophysical Research*, 106, 7193-7210. <http://doi.org/10.1029/2000JD900547>  
11  
12 560 Soja, A. & Groisman, P. (2018). Earth Science and the integral climatic and socio-economic  
13 561 drivers of change across northern Eurasia: the NEESPI legacy and future direction.  
14 562 *Environmental Research Letters*, 13(4), 040401. [http://doi.org/10.1088/1748-](http://doi.org/10.1088/1748-9326/aab834)  
15 563 [9326/aab834](http://doi.org/10.1088/1748-9326/aab834)  
16  
17 564 Son, H.-Y., Park, W., Jeong, J.-H., Yeh S.-W., Kim, B.-M., Kwon, M. & Kug, J.-S. (2012).  
18 565 Nonlinear impact of the Arctic Oscillation on extratropical surface air temperature,  
19 566 *Journal of Geophysical Research: Atmospheres*, 117, D19102.  
20 567 <http://doi.org/10.1029/2012JD018090>  
21  
22 568 Suo, L., Tan, B. & Huang, J. (2009). Further exploration on causes of temperature anomalies  
23 569 associated with the abnormal northern annular mode. *Chinese Science Bulletin*, 54(12),  
24 570 2101-2106. <https://doi.org/10.1007/s11434-009-0045-2>.  
25  
26 571 Thompson, D. W. J. & Wallace, J. M. (1998). The Arctic Oscillation signature in the wintertime  
27 572 geopotential height and temperature fields. *Geophysical research letters*, 25(9), 1297-  
28 573 1300. <https://doi.org/10.1029/98GL00950>.  
29  
30 574 Thompson, D. W. J. & Wallace, J. M. (2000). Annular modes in the extratropical circulation.  
31 575 Part I: Month-to-month variability. *Journal of climate*, 13(5), 1000-1016.  
32 576 [https://doi.org/10.1175/1520-0442\(2000\)013<1018:AMITEC>2.0.CO;2](https://doi.org/10.1175/1520-0442(2000)013<1018:AMITEC>2.0.CO;2).  
33  
34 577 Thompson, D. W. J., Wallace, J. M. & Hegerl, G. C. (2000). Annular Modes in the  
35 578 Extratropical Circulation. Part II: Trends. *Journal of climate*, 13(5), 1018-1036.  
36 579 [https://doi.org/10.1175/1520-0442\(2000\)013<1018:AMITEC>2.0.CO;2](https://doi.org/10.1175/1520-0442(2000)013<1018:AMITEC>2.0.CO;2).  
37  
38 580 Thompson, D. W. J. & Wallace, J. M. (2001). Regional climate impacts of the Northern  
39 581 Hemisphere annular mode. *Science*, 293(5527), 85-89.  
40 582 <http://doi.org/10.1126/science.1058958>.  
41  
42 583 Wilks, D. S. (1995). *Statistical Methods in the Atmospheric Sciences*. Second Edition. Elsevier  
43 584 Academic Press: San Diego, CA.  
44  
45 585 Wilks, D. S. (1997). Resampling Hypothesis Tests for Autocorrelated Fields, *Journal of*  
46 586 *Climate*, 10(1), 65-82. [https://doi.org/10.1175/1520-](https://doi.org/10.1175/1520-0442(1997)010<0065:RHTFAF>2.0.CO;2)  
47 587 [0442\(1997\)010<0065:RHTFAF>2.0.CO;2](https://doi.org/10.1175/1520-0442(1997)010<0065:RHTFAF>2.0.CO;2)  
48  
49 588 Woo, S.-H., Kim, B.-M., Jeong, J.-H., Kim, S.-J., & Lim, G.-H. (2012). Decadal changes in  
50 589 surface air temperature variability and cold surge characteristics over northeast Asia  
51 590 and their relation with the Arctic Oscillation for the past three decades (1979–2011), *J.*

- 1  
2  
3  
4 591 *Geophys. Res.*, 117, D18117. <http://doi.org/10.1029/2011JD016929>.
- 5  
6 592 Wu, B., Zhang, R. & D'Arrigo, R. (2006). Distinct modes of the East Asian winter monsoon.  
7 593 *Monthly weather review*, 134(8), 2165-2179. <https://doi.org/10.1175/MWR3150.1>
- 8  
9 594 Xu, M., Xu, H. & Ma, J. (2016). Responses of the East Asian winter monsoon to global  
10 595 warming in CMIP5 models. *International Journal of Climatology*, 36(5), 2139-2155.  
11 596 <https://doi.org/10.1002/joc.4480>
- 12  
13 597 Zhang, Y., Sperber, K. R., & Boyle, J. S. (1997). Climatology and Interannual Variation of the  
14 598 East Asian Winter Monsoon: Results from the 1979–95 NCEP/NCAR Reanalysis,  
15 599 *Monthly Weather Review*, 125(10), 2605-2619. [https://doi.org/10.1175/1520-0493\(1997\)125<2605:CAIVOT>2.0.CO;2](https://doi.org/10.1175/1520-0493(1997)125<2605:CAIVOT>2.0.CO;2)
- 16  
17 600  
18 601 Zhou, J. & Tung, K. (2013). Deducing Multidecadal Anthropogenic Global Warming Trends  
19 602 Using Multiple Regression Analysis. *Journal of the Atmospheric Sciences*, 70(1), 3-8,  
20 603 <https://doi.org/10.1175/JAS-D-12-0208.1>  
21  
22  
23  
24 604  
25  
26  
27  
28  
29  
30  
31  
32  
33  
34  
35  
36  
37  
38  
39  
40  
41  
42  
43  
44  
45  
46  
47  
48  
49  
50  
51  
52  
53  
54  
55  
56  
57  
58  
59  
60